

Effects of Null Mutations and Overexpression of Capping Protein on Morphogenesis, Actin Distribution and Polarized Secretion in Yeast

James F. Amatruda, David J. Gattermeir, Tatiana S. Karpova, and John A. Cooper

Department of Cell Biology and Physiology, Washington University School of Medicine, St. Louis, Missouri 63110

Abstract. *CAP1*, the gene encoding the α subunit of *Saccharomyces cerevisiae* capping protein, was cloned using a probe prepared by PCR with primers based on the amino acid sequence of purified α subunit peptides. The sequence is similar to that of capping protein α subunits of other species but not to that of the *S. cerevisiae* capping protein β subunit or any other protein.

Null mutants of capping protein, prepared by deletion of the coding region of *CAP1* and *CAP2* separately or together, are viable and have a similar phenotype. Deletion of the gene for one subunit leads to a loss of protein for the other subunit. The null mutant has a severe deficit of actin cables and an increased number of actin spots in the mother. Cells are round and rela-

tively large. These features are heterogeneous within a population of cells and vary with genetic background. Overexpression of *CAP1* and *CAP2* also causes loss of actin cables and cell enlargement, as well as the additional traits of aberrant morphogenesis and cell wall thickening. Capping protein null strains and overexpression strains exhibited normal polarized secretion during bud growth as demonstrated by labeling with fluoresceinated Con A. Projection formation and chitin deposition in response to mating pheromone, mating efficiency, and bud site selection were also normal in capping protein null strains. In addition, bulk secretion of invertase was unimpaired. These data indicate that actin cables are not required for polarized secretion in *S. cerevisiae*.

THE yeast *Saccharomyces cerevisiae* exhibits polarized growth and morphogenesis in a variety of ways during its life cycle (14). Budding begins with the non-random selection of a bud site at one pole of the cell. As the cell cycle proceeds, growth is asymmetric; the bud enlarges selectively while the mother cell grows little (28). At the end of budding the mother and bud are separated by a chitinous septum that grows across the bud neck and is accompanied by new cell wall growth specifically targeted to this region. Another example of polarized growth occurs in haploid yeast exposed to mating pheromone; these cells form a projection, and chitin is deposited at the base of the projection. Cells can mate selectively with specific partners within a population, which implies that polarization can occur in a specific direction (33).

Polarized growth results from the selective deposition of newly synthesized cell wall components in areas of growth such as the bud tip, as shown by fluorescent (55) or radioactive (24) labeling of cell wall components. The secretory enzymes invertase (56) and acid phosphatase (25) are also selectively targeted to the growing bud. Cell surface growth and protein export are impaired in mutants which accumulate intracellular vesicles, showing that both processes depend on vesicle secretion (41).

Several lines of evidence suggest that the yeast actin

cytoskeleton may mediate polarized growth. Strains with *ts* alleles of *ACT1*, the yeast actin gene, exhibit impaired secretion and mislocalization of chitin deposition after a short time at the restrictive temperature (42). While bulk secretion is normal, internal stores of the secretory enzyme invertase accumulate in these strains, suggesting that polarized secretion is impaired. Strains with a *ts* allele of the *MYO2* gene, which encodes a putative actin-based motor, do not initiate bud formation at the restrictive temperature, although bulk secretion is unaffected and the cell cycle, including the growth of existing buds, proceeds through cytokinesis (36).

Several different forms of actin may be morphologically distinguished in yeast. Cortical actin spots (also called "actin dots" or "actin patches"—the three terms are synonymous) assemble at the incipient bud site and later cluster at the tip of the growing bud. In contrast, mother cells contain actin cables oriented generally parallel to the mother bud axis, as well as a few actin spots. Shortly before cell division, cables disappear and the mother acquires actin spots. Cell division is accompanied by the appearance of an actin ring at the bud neck (1, 37), which is not a cluster of spots (6). Actin spots are also seen at the tips of projections formed by cells exposed to mating pheromone. Some (29, 39) but not other (8) studies have found that these cells have cables, which are oriented toward the projection.

The role of the cables is unknown. Because they are oriented parallel to the mother-bud axis, an intriguing possibility is that the cables mediate polarized growth and secretion (1, 20, 21, 37). Cables probably represent bundles of actin filaments (1), and in other systems myosin-coated vesicles move along actin filaments, leading to the hypothesis that in yeast secretory vesicles follow actin cables to their site of insertion as a molecular mechanism of polarized secretion (20, 22, 36). On the other hand, the location of cortical actin spots correlated with sites of new cell wall growth (1); therefore spots may mediate polarized secretion.

We have tested these hypotheses by studying polarized secretion in strains that are deficient in actin cables in response to null mutations or overexpression of capping protein, a ubiquitous actin-binding protein. These strains exhibit minimal or no defects in polarized secretion as evaluated by several criteria, which argues that actin cables are not required for polarized secretion in yeast.

Materials and Methods

Materials and Supplies

Unless otherwise noted, chemicals were from Sigma Chemical Co. (St. Louis, MO) and materials and solvents from Fisher Scientific (St. Louis, MO).

Yeast Strains and Genetic Techniques

Yeast strains used are listed in Table I. Media and techniques of crossing,

sporulation, tetrad dissection, transformation, and preparation of genomic DNA were as described (46). For experiments in which the effects of ethylene glycol were tested, 1 or 2 M ethylene glycol was included in the YPD medium.

Proteins

SDS-PAGE, immunoblots, preparation of affinity-purified rabbit anti-yeast capping protein antibodies, purification of yeast capping protein, separation of α and β subunits, endoproteolytic digestion, and NH₂-terminal amino acid sequencing were as described (6).

DNA Sequencing and Sequence Analysis

DNA was sequenced with the chain termination method (48) using modified T7 DNA polymerase (United States Biochemical, Cleveland, OH). Both strands of clone λ 1 were sequenced, using subclones created by sonication of the original insert. Multiple sequence alignments were generated using GAP (19). The nucleotide sequence of clone λ 1 and its complement were searched against the EMBL and GenBank nucleotide databases using FASTA (43). The predicted amino acid sequences of the *CAP1* gene and the ORF were searched versus the GenPept and SWISS-PROT protein sequence databases using FASTA, and versus the SWISS-PROT and PIR databases using BLAST (4).

PCR Amplification of a *CAP1* Coding Sequence Fragment

NH₂-terminal amino acid sequence data from peptides A3 and A7 were used to design degenerate oligonucleotides A7/FOR, A3/REV, A3/FOR, and A7/REV (Table II). Oligonucleotides were used in pairs (A7/FOR with A3/REV; A3/FOR with A7/REV) in a PCR reaction using 100 ng yeast genomic DNA. The reaction consisted of 40 cycles of 30 s at 94°C, 30 s at 35°C, and 30 s at 72°C. Only the A7/FOR and A3/REV primer pair yielded amplified products.

Table I. Yeast Strains Used in This Study

YJC Number	Other name	Relevant genotype	Source
075	JC482	MATa <i>CAP1 CAP2</i>	K. Tatchell*
076	KT607	MAT α <i>CAP1 cap2-1::URA</i>	K. Tatchell
078	KT903	MATa <i>CAP1 cap2-1::URA3</i>	K. Tatchell
082	YM702	MAT α <i>CAP1 CAP2</i>	M. Johnston [‡]
085		MAT α <i>CAP1 cap2-Δ1::HIS3</i>	This laboratory
093	W303-1A	MATa <i>CAP1 CAP2</i>	R. Rothstein [§]
095	YPH501	MATa <i>CAP1 CAP2</i> MAT α <i>CAP1 CAP2</i>	P. Hieter
097	DC14	MATa <i>his6</i>	K. Blumer [‡]
163	W303	MATa <i>CAP1 CAP2</i> MAT α <i>CAP1 CAP2</i>	This laboratory
165		MATa <i>CAP1 cap2-Δ1::HIS3</i> MAT α <i>CAP1 cap2-1::URA3</i>	This laboratory
174		MAT α <i>cap1-Δ1::TRP1 CAP2</i>	This study
285		MATa <i>leu2-3, 112 [pABZ259]</i>	This study
288		MATa <i>leu2-3, 112 [pBJ114]</i>	This study
365	AAY1024	MAT α <i>CAP1 CAP2</i>	A. Adams**
384		MATa <i>cap1-Δ1::TRP1 cap2-Δ1::HIS3</i>	This study
388		MAT α <i>CAP1 CAP2</i>	This study
389		MATa <i>CAP1 cap-2Δ1::HIS3</i>	This study
390		MATa <i>cap1-Δ1::TRP1 CAP2</i>	This study
391		MAT α <i>cap1-Δ1::TRP1 cap2-Δ1::HIS3</i>	This study
447		MAT α <i>CAP1 cap2-Δ1::LEU2</i>	This laboratory
598	AAY1219	MATa <i>CAP1 cap2-Δ1::HIS3</i>	A. Adams/D. Drubin ^{‡‡}
599	AAY1236	MATa <i>CAP1 cap2-Δ1::HIS3</i>	A. Adams/D. Drubin
600	AAY1232	MAT α <i>CAP1 CAP2</i>	A. Adams/D. Drubin

* North Carolina State University, Raleigh, NC.

[‡] Washington University, St. Louis, MO.

[§] Columbia University, New York.

^{||} Johns Hopkins University, Baltimore, MD.

** University of Arizona, Tucson, AZ.

^{‡‡} University of California, Berkeley, CA.

Table II. Sequences of Proteolytic Peptides and Oligonucleotides

Name	Sequence	Position in Cap 1p sequence (residue numbers)
Peptides		
A7	FF(N/D)PVNSVIFSVNHLERK	75–92
A3	GLDIEPYEFTHAK	93–105
A6	INXGSAIGFYXLG	249–261
Oligonucleotides (5' to 3')		
A7/FOR	CC(A/C/T)GT(C/T)AA(C/T) TC(G/A/T/C)GT(C/T)AT (C/T)TT(C/T)CA(C/T)GT (C/T)AA	
A3/REV	(T/C)TT(T/G/A)GC(G/A) TG(G/A)AA(T/C)TC(G/A) TA(T/G/A)GG(T/C)TC (G/A)AT	
A3/FOR	AA(A/G)GG(C/G/T)(C/T)T (A/C/T)GA(C/T)AT(C/T)GA (A/G)CCATA(C/T)GA(A/G) TT	
A7/REV	A(G/T)(G/T/A)GC(G/A)TT (G/A)AC(G/A)TG(G/A)AA (G/A)AC(G/A/T/C)GA(A/G) TT	
CAP1/Exact	AACCATTTAGAGCGCAAG- GGCCTTGACAT	

Cycles in which no amino acid residue could be assigned are indicated by "X." Positions of nucleotide degeneracy are indicated by parentheses.

Four amplified bands were subcloned into pBluescript (Stratagene, La Jolla, CA) and sequenced. One product correctly predicted the amino acid sequences of peptides A3 and A7, which by coincidence are immediately adjacent to each other in the primary sequence.

Library Screening and Sequencing

Standard molecular techniques were used (47). The sequence of the PCR product was used to design the non-degenerate oligonucleotide CAP1/Exact (Table II), which was used to screen a randomly sheared yeast genomic DNA library in λ gt11 (23). 40,000 phage were screened, yielding six positives. Digestion of purified phage DNA (31) with EcoRI produced inserts from five of these phage (see Fig. 1), which were subcloned and analyzed by restriction digest and sequence. To sequence both strands of clone λ 1 in its entirety, the insert DNA was purified and sonicated to produce 100–300-bp fragments, which were subcloned and sequenced. Several synthetic oligonucleotides were used to complete the sequence.

Physical Mapping of the CAP1 Gene

The λ EcoRI inset was 32 P-labeled with random primers and used to screen the M. V. Olson lab filter set, kindly provided by Linda Riles (Washington University, St. Louis, MO). The presence of CAP1 on the identified phage was confirmed by purifying and partially sequencing the phage insert DNA (31).

Disruption of the CAP1 Gene

90% of the coding region of CAP1 was disrupted in diploid strain YJC163 by γ -loop mutagenesis as described (54). The 5' EcoRI-ScaI and 3' BglII-EcoRI restriction fragments flanking the CAP1 gene were subcloned into BamHI-SmaI cut pRS304. The recombinant plasmid was digested with EcoRI and used to transform yeast to tryptophan prototrophy by the lithium acetate method (46). Sporulation gave rise to four viable spores, with 2:2 segregation of the Trp⁺ marker. *cap1* Δ *cap2* Δ mutants were created by

crossing *cap1* Δ and *cap2* Δ strains and sporulating the resulting heterozygous diploid.

Fluorescence Microscopy

Cells were fixed for fluorescence microscopy and stained with rhodamine-phalloidin to detect actin or with Calcofluor to detect chitin as described, except that rhodamine-phalloidin was at 3.3 μ M (2, 44, 45). Anti-actin staining was as described (22), using affinity-purified rabbit anti-yeast actin antibodies generously provided by David Drubin (University of California, Berkeley, CA). α -factor treatment was as described (6). The mounting solution contained 1 mg/mL *p*-phenylenediamine to inhibit bleaching. Cells were observed with a 100 \times N.A. 1.3 Plan-Neofluar objective on an Axiovert 10 microscope (Carl Zeiss, Oberkochen, Germany) equipped for epifluorescence microscopy with a 50 W mercury arc lamp or an AxioPhot with a 100 W lamp, and photographed on T-Max 400, T-Max 100, and Tech-Pan Film (Eastman Kodak Co., Rochester, NY) as appropriate.

Con A Staining

Cells were grown in 10 mL YPD (46) with 2% glucose to an OD₆₀₀ of \sim 1.0, harvested, washed in labeling buffer (10 mM Tris, pH 7, 100 mM NaCl, 2 mM CaCl₂, 2 mM MnCl₂) and resuspended in 1 mL labeling buffer. FITC-conjugated Con A (Molecular Probes, Eugene, OR) was added to a final concentration of 0.1 mg/mL, and the cultures were incubated 20 min in the dark at room temperature. The cells were harvested, resuspended in 20 mL YPD with 0.1% glucose and incubated 30–120 min at 30°C with agitation. Aliquots were removed, sonicated, washed once in 10 mM NaN₃, mounted on slides, and observed by fluorescence microscopy.

Overexpression of Capping Protein

The 2.8-kb EcoRI insert from λ 1 was cloned into pBluescript, creating plasmid pBJ060. An AflIII site was created 2 bp 5' of the initiating ATG of the CAP1 gene in pBJ060 by oligonucleotide-directed, site-specific mutagenesis (38). The entire coding sequence of CAP1 was sequenced to ensure that no additional mutations had been created by the procedure. Digestion of pBJ060 with AflIII yielded a 1.2-kb product which was blunt-ended and ligated into EcoRV-cut pBluescript, creating pBJ093. pBJ093 was digested with EcoRI and SalI to release a 1.1-kb CAP1 coding region cassette.

To create a CAP2 coding region cassette, plasmid pBJ010 containing CAP2 with an artificial 5' BamHI site (described in reference 5) was digested with BamHI and SspI and the 870-bp insert was purified and ligated into BamHI/SmaI cut pBluescript, creating plasmid pBJ094. Digestion of pBJ094 with BamHI and SalI released a 900-bp CAP2 cassette.

A 685-bp BamHI-EcoRI fragment containing the GAL1 and GAL10 promoters was prepared from plasmid pBM258 (M. Johnston, Washington University, Department of Genetics, St. Louis, MO). This fragment was ligated with the CAP1 and CAP2 coding region cassettes, the ligation products were digested with SalI, and the 2.7-kb fragment containing CAP2-GAL1/GAL10-CAP1 was gel purified and ligated into SalI cut pABZ259 (10) to create plasmid pBJ114.

Yeast strain YJC093 was transformed with pABZ259 or with pBJ114 to create strains YJC285 and YJC288, respectively. To induce overexpression of CAP1p and CAP2p, YJC285 and YJC288 were grown overnight in synthetic –Leu medium with 2% glucose (46), diluted to an OD₆₀₀ of 0.5 in synthetic –Leu medium with 2% lactate and 2% pyruvate, and grown 2 h at 30°C. Galactose was added to a final concentration of 2%, and growth was continued for 6–8 h at 30°C.

EM

Growth, fixation, and embedding of cells were as described (57, 58). Cells were embedded in LR White resin, sectioned, stained with 1% uranyl acetate followed by lead citrate, and observed on a Zeiss EM10 electron microscope.

Mating Efficiency

5×10^6 cells of strain YJC388 (MAT α CAP1 CAP2) or YJC391 (MAT α *cap1* Δ 1::TRP1 *cap2* Δ 1::HIS3) were mixed with an equal number of cells of strain YJC097 (MAT α His6), harvested on filters and incubated on solid medium as described (34). After 2.5 h at 30°C cells were removed from

the filters, diluted 10³-fold in H₂O and plated on solid YPD. Colonies appearing on these plates were replicated to synthetic minimal medium and to synthetic -Leu medium to identify diploids and MAT α haploids, respectively. Similar results were obtained when cells from the filter were plated directly onto synthetic minimal medium.

Invertase Secretion

Invertase secretion was assayed as described (9), except that all cultures were grown at 30°C, and time 0 was the time of shift to 0.1% glucose. External invertase activity was defined as the activity in non-permeabilized samples; total invertase activity as the activity in samples permeabilized by Triton X-100 treatment and freeze-thawing; and internal invertase activity as total external. The OD₆₀₀ of the non-permeabilized samples was used to normalize the data. Triplicate determinations were made for each time point. One unit of invertase activity was defined as 1 nmol glucose produced/([min at 30°C] [1.0 A₆₀₀ U]).

Results

Cloning of *CAP1*

Previously we purified yeast capping protein (6) and cloned *CAP2*, the gene encoding the β subunit (5). To clone *CAP1*, the α subunit gene, NH₂-terminal amino acid sequence from two α subunit peptides (6) was used to design degenerate oligonucleotides for use in a PCR reaction with yeast genomic DNA as the template (Table II). One amplified product correctly predicted the amino acid sequence of the two peptides and was used to design a non-degenerate *CAP1* oligonucleotide for library screening. Five non-identical positive clones were isolated from a randomly sheared genomic DNA library in phage λ gt11 (Fig. 1). The sequence of clone λ 1 was determined and contains an 804-bp open reading frame which we name *CAP1* and propose encodes the α subunit of capping protein. To conserve space, the sequence is not shown but can be found in GenBank and EMBL databases under accession number X61398. The three α subunit peptide sequences are present in the amino acid sequence predicted from *CAP1* (Table II). In addition, the amino acid composition of the purified α subunit is identical, within error, to that predicted by *CAP1*, and the relative molecular weight observed by SDS-PAGE is identical, within error, to that predicted (data not shown). The coding region of *CAP1* is preceded by a stop site in frame with the initiating methionine at 12-bp upstream, preceded by a TATA box 70-bp upstream and followed by transcription termination sequences 60–500-bp downstream.

The predicted amino acid sequence of the protein encoded by *CAP1* (Cap1p) is similar to the predicted amino acid sequences of capping protein α subunits from *Dictyostelium*, chicken, frog, and dog (Fig. 2). Over its entire length, Cap1p is 32 and 27% identical to the capping protein α subunits from chicken and *Dictyostelium*, respectively (13, 27). Searches of the *CAP1* nucleotide and protein sequences against the GenBank, EMBL, GenPept, PIR, and SWISS-PROT databases did not reveal any other similar sequences.

CAP1 was physically mapped to chromosome XI, between the centromere and *PUT3* (40), by hybridization of the λ 1 insert to the M. V. Olson lab filter set. *CAP1* is found in MERG 0919, λ #6578, which was confirmed by isolation and partial sequence of the phage DNA, and is probably on group 33, based on the restriction digest pattern. The data do not indicate the orientation of the gene on this group.

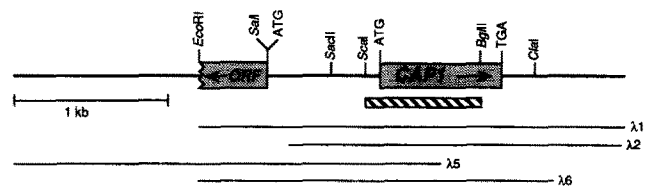


Figure 1. Physical map of the *CAP1* gene. The relative positions of five phage λ inserts identified by library screening are shown. The nucleotide sequence of clone λ 1 was determined and is in the GenBank and EMBL databases, accession number X61398. Restriction sites are derived from the nucleotide sequence, which does not include the region to the left of the EcoRI site. The hatched bar is the region deleted in the *cap1- Δ* allele. (ORF) Open reading frame present at the 5' end of clone λ 1. The sequence of the ORF was not completed; searches of the database with the partial predicted amino acid sequence revealed no similar sequences. The indicated EcoRI site is a bona fide genomic site; otherwise each phage has at its ends EcoRI sites derived from the library construction.

S.c.	MSSSKFPEVYINKIINDSPGPELREVVYDDIKITSENSLKNFTI	50
D.d.	MASNOELVQIARNFLINAPPSEFVEVSDVRLLESSELNANSA	44
X.l.NEVFNDVRLLLNNDNLLREGA	21
G.g.1	MADLEEDVSDEEKVRIAIAKFIHAPPGEFNEVFNDVRLLLNNDNLLREGA	50
G.g.2	MADLEEQLSDEEKVRIAIAKFIHAPPGEFNEVFNDVRLLLNNDNLLREGA	50
C.f.	MADLEEQLSDEEKVRIAIAKFIHAPPGEFNEVFNDVRLLLNNDNLLREGA	50
Con.	S PP E EV D	
S.c.	LDATENYVNCIPTEVNGNSVITISKYKNGAKFDFPNSVITFSVNH	100
D.d.	GSTPFREYNTSOMVSVQNSKSGSLITKGEISNNEVLDPNKQVITVDH	92
X.l.	AHAFAYQYMDQFTPKIEGYDDQVLITEHGDGNGRFLDPNKKISFKFDH	71
G.g.1	AHAFAYQYMDQFTPKIEGYDDQVLITEHGDGNGRFLDPNKKISFKFDH	100
G.g.2	AHAFAYQYMDQFTPKIEGYDDQVLITEHGDGNGRFLDPNKKISFKFDH	100
C.f.	AHAFAYQYMDQFTPKIEGYDDQVLITEHGDGNGRFLDPNKKISFKFDH	100
Con.	YN I DP N H	
S.c.	LRRKGDHNPYBETHAKIEKQGLKELDHLHEYLHSEFPEDVSEAVYVPE	150
D.d.	IKCEITGERSASGETEOLIEQYRAAFDEATHYCNDFYPNVGVSVYGGK	141
X.l.	LRKEASDPPHPDDSNALKSWRDACDALARAYVKEHYPNVGVSVYGGK	118
G.g.1	LRKEASDPPHPDDSNALKSWRDACDALARAYVKEHYPNVGVSVYGGK	147
G.g.2	LRKEATDPPRPEVENAIESWRNSVETALRAYVKEHYPNVGVSVYGGK	147
C.f.	LRKEATEPPRPEVENAVESWRNSVETALRAYVKEHYPNVGVSVYGGK	147
Con.	Y P VY	
S.c.	LEESKISLITVSTYVNNFNWNGWRSSVYVLEDPRELSGOST	200
D.d.	VSEGIKIVCISICHVYVNFYFSGWRSSVWCTEPELSENVSNVGAIVAV	190
X.l.	IDGQQTIVSCIESHQPQKFNWNGRWRSEWKFITSPSTAQVAAGVLKI	165
G.g.1	IDGQQTIIACIESHQPQKFNWNGRWRSEWKFITSPSTAQVAAGVLKI	194
G.g.2	IDGQOITIIACIESHQPQKFNWNGRWRSEWKFITSPSTQVAAGILKI	194
C.f.	IDGQOITIIACIESHQPQKFNWNGRWRSEWKFITSPSTQVAAGILKI	194
Con.	I I F G WRS	
S.c.	QVHYEDGNVSESSKRDINGSNVDDVVCITSDIERNFNEFL	250
D.d.	NVHYEDGNVOLNVTOKQETSSESDAQSTANAFKAIERAEINLHTAL	239
X.l.	QVHYEDGNVOLVSHKDIQDSYVVSQVDTAKEFKIKIENAEYQYTAI	214
G.g.1	QVHYEDGNVOLVSHKDIQDSYVVSQVDTAKEFKIKIENAEYQYTAI	243
G.g.2	QVHYEDGNVOLVSHKDIQDSLTVSNEAQTAKEFKIKIENAEYQYTAI	243
C.f.	QVHYEDGNVOLVSHKDIQDSLTVSNEAQTAKEFKIKIENAEYQYTAI	243
Con.	VHY EDGNV S E	
S.c.	DLSEFDLNEKFKALRRRLPVTTRKIDWKNILSYKIGKEMQNA	300
D.d.	DNYSTAGDTTFKALRRRLPVTTRKIDWKNVSEFKIANELAK	281
X.l.	SENYQTMDSDTTFKALRRRLPVTTRKIDWKNILSYKIGKEMQNA	257
G.g.1	SENYQTMDSDTTFKALRRRLPVTTRKIDWKNILSYKIGKEMQNA	286
G.g.2	SENYQTMDSDTTFKALRRRLPVTTRKIDWKNILSYKIGKEMQNA	286
C.f.	SENYQTMDSDTTFKALRRRLPVTTRKIDWKNILSYKIGKEMQNA	286
Con.	FKALRR LP R K I W	

Figure 2. Comparison of the amino acid sequence of capping protein α subunits. Alignment of the predicted protein sequences of capping protein α subunits from *S. cerevisiae* (S.c.), *Dictyostelium discoideum* (D.d.) (27), *Xenopus laevis* (X.l.) (7), *Gallus gallus* α 1 and α 2 (G.g.1 and G.g.2) (13, 17) and *Canis familiaris* (C.f.) (Zopf and Walter, 1990, unpublished data). (Con.) Consensus line showing residues identical in all six sequences. Two or more identical residues are shown in inverse black; two or more similar residues (26) are shown in inverse gray.

Phenotype of Null Mutants

CAP1 was deleted by homologous recombination in a diploid wild-type strain. Sporulation and tetrad dissection yielded four viable spores, indicating that *CAP1* is not an essential gene. Crossing of *cap1Δ* and *cap2Δ* strains and sporulation of the resulting heterozygous diploid indicated that *cap1Δ-cap2Δ* double mutant strains are also viable. *cap2Δ* mutants are viable but grow ~25% slower than wild-type strains in YPD medium at 30°C (5). When 1 M ethylene glycol was added to the solid YPD medium, *cap2Δ* strains but not isogenic wild-type strains ceased growth at 39°C. In the presence of 2 M ethylene glycol this effect was seen at 34°C.

Immunoblot analysis of *cap1Δ*, *cap2Δ* and *cap1Δcap2Δ* strains using polyclonal anti-capping protein antibodies indicated that all strains showed reduced levels of both capping protein subunits relative to wild-type. No capping protein bands are present in *cap1Δ* or *cap1Δcap2Δ* strains, and only a small amount of Caplp persists in *cap2Δ* strains (Fig. 3). Thus, *cap1Δ*, *cap2Δ*, and *cap1Δcap2Δ* strains all lack functional capping protein. Consistent with this result, we find no phenotypic differences between these strains.

Deletion of either or both capping protein subunits causes cells to become enlarged and rounded (Fig. 4). Nearly all mutant cells are round, as compared to wild-type cells, which are oval. Only a fraction of the mutant population is enlarged; many cells of normal size are found.

The actin distribution was examined by fluorescence microscopy with fluorescent phalloidin and anti-actin antibodies. Mother cells have a severe deficit in actin cables. Wild-type strains generally show 80–90% of cells with several cables, which run the length of the cell. In most backgrounds (YJC076, YJC085, YJC174, and YJC384; derived from strains YJC075, YJC082, YJC095, and YJC163, respectively), only 1 to 10% of null mutant mother cells contain cables, and cables in those cells are generally, but not always, less numerous, less intense, and shorter than those of wild-type cells (Fig. 4). Staining with anti-actin antibodies was superior to fluorescent phalloidin in detection of cables. This difference was most noticeable in one background (YJC598-600), in which a significantly higher fraction (30–50%) of null mutant cells had cables detected by anti-actin but only 5% had cables detected by fluorescent phalloidin. The most likely possibility for these results is simply that the anti-actin protocol, which notably includes extraction and flattening of cells leading to a much reduced background, is more sensi-

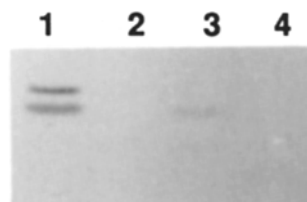


Figure 3. Immunoblot of wild-type and capping protein null strains. Total yeast lysates were electrophoresed, blotted, and probed with an affinity-purified anti-yeast capping protein antibody that recognizes both subunits of capping

protein (6). (Lane 1) YJC388 (wild-type); (lane 2) YJC390 (*cap1Δ*); (lane 3) YJC389 (*cap2Δ*); (lane 4) YJC391 (*cap1Δcap2Δ*). Only the 30-kD region of the blot is shown to conserve space; no other bands were seen, as documented previously (6). This experiment was also performed with affinity-purified antibodies specific for each subunit, and gave similar results, which are not shown to conserve space.

tive, but we have not excluded the possibility that some of the cables detected by anti-actin do not bind phalloidin. The protocols for the two reagents are mutually exclusive and do not permit a double label experiment.

Null mutants lacking cables generally show an increased number of cortical actin spots distributed diffusely over the surface of the mother cell as well as the bud, whereas in wild-type cells these spots are predominantly clustered at the tip of the bud (Fig. 4). This phenomenon was also heterogeneous within a population and between different genetic backgrounds. The lack of cables did correlate with increased numbers of diffuse dots.

Overexpression of Capping Protein

Having found that cells lacking capping protein have an altered actin cytoskeleton, we tested the effect of capping protein overexpression. Because expressed single subunits of capping protein from other systems have little or no activity in actin polymerization assays in vitro (30, 32) and we suspect that single subunits are unstable based on the results above, we simultaneously overexpressed both subunits. Transformation of yeast with a vector in which both the *CAP1* and *CAP2* genes are placed under the control of the divergent *GALI-GAL10* promoters led to a >200-fold overproduction of the protein when the cells were grown on media containing galactose as assessed by quantitative immunoblot analysis of cell lysates (data not shown). As a control we examined cells transformed with the parent vector lacking the *CAP1* and *CAP2* genes.

Overexpression of capping protein led to a minor deficit in growth on solid synthetic media that selects for the plasmid and contains galactose (2%) and raffinose (2%) as the carbon source (data not shown). This experiment could not be performed with rich glucose-containing medium, which would be interesting since strains deleted for *SAC6*, another actin-binding protein, are Ts⁻ for growth at 37°C on rich but not selective media (3).

The morphology of the cells in the overexpressing population is also heterogeneous. Some have thickened cell walls and/or buds with unusual shapes, and some are normal (Fig. 5). Thin-section EM confirmed that the cell walls are thick in many of these cells (data not shown). Second, overexpression causes a decrease in the number of cells containing a normal actin cytoskeleton. 5% (9/200) of cells overexpressing capping protein contain actin cables, compared with 86% (172/200) of control cells (representative cells shown in Fig. 5). Both small and large cells exhibit disrupted actin cytoskeletons and altered bud morphology. Those few cells that do contain actin cables generally have normal size and bud morphology; however given the small numbers of such cells it is difficult to draw strong conclusions about the correlation between aberrant cell morphology and the loss of actin cables.

Polarized Secretion

To test the hypothesis that actin cables are important for polarized secretion, polarized growth of capping protein null, and overexpressing strains, which are deficient in actin cables, was tested in several different assays. First, we used fluorescent Con A to differentially label pre-existing and newly synthesized cell surface molecules. Because the for-

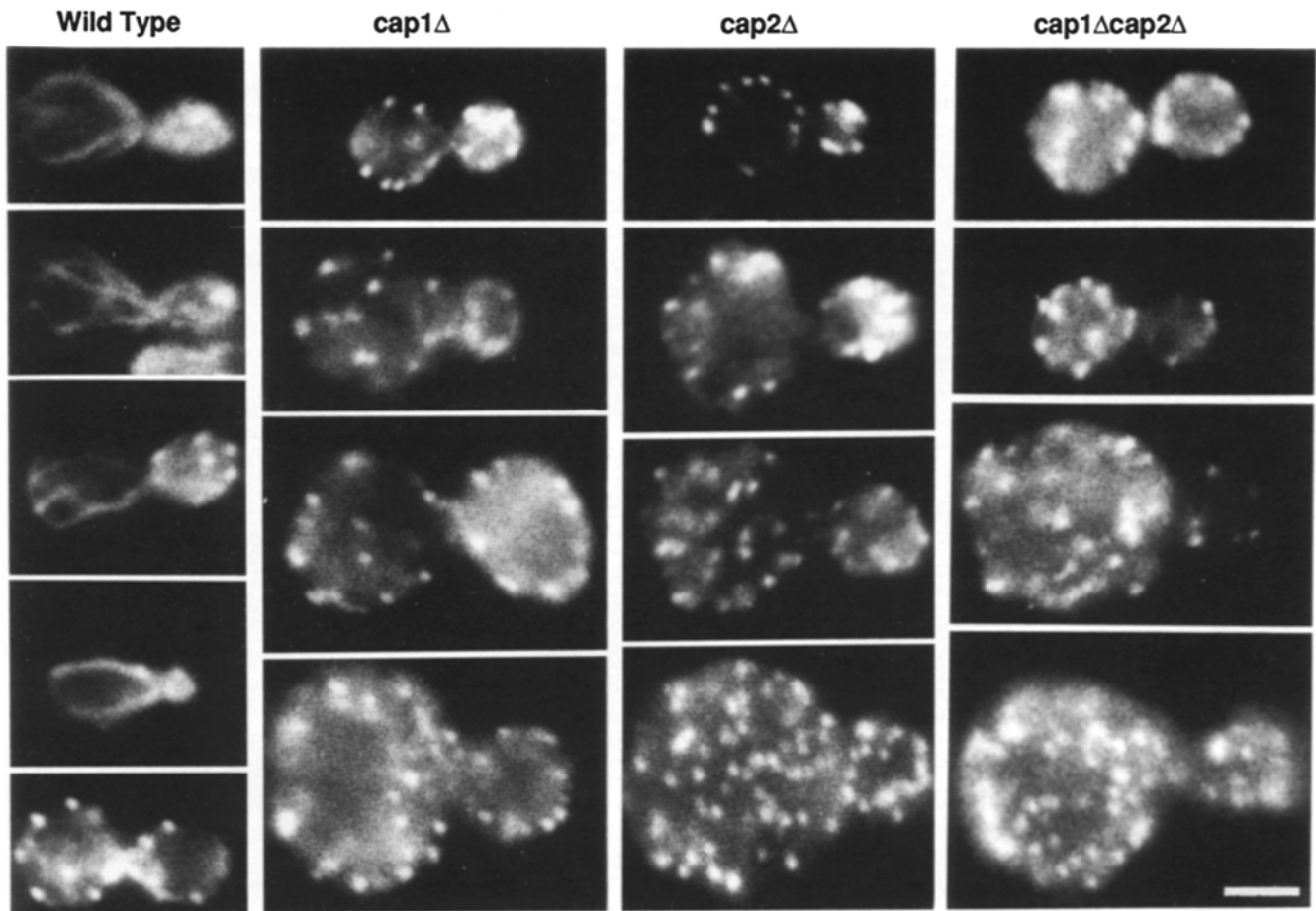


Figure 4. Actin distribution in wild-type and capping protein null strains. Cells were fixed and stained with rhodamine-conjugated phalloidin. Cells representing the bulk of the population are shown, but as discussed in the text, the mutant population includes a small percentage of cells that resemble wild-type, which are more noticeable when staining with anti-actin instead of phalloidin. The cell at the bottom of the wild-type panel lacks cables, a normal finding for cells near cytokinesis. (*Wild-Type*) YJC388; (*cap1Δ*) YJC390; (*cap2Δ*) YJC389; (*cap1Δ cap2Δ*) YJC391. Bar, 3 μ m.

mation of new cell wall is monitored directly, this is a direct test for polarized growth. Second, we used the fluorescent dye Calcafluor (primulin) to label chitin, a cell wall component that is specifically deposited at the bud neck. Third, we examined polarization in response to mating pheromone, including projection formation and chitin deposition at the base of the projection. Fourth, we assessed mating efficiency and mating partner discrimination, indirect measures of cell polarity. Finally, we examined invertase secretion, as an example of bulk secretion that is not necessarily polarized.

Cell Surface Growth

Newly synthesized cell-wall components including mannoproteins (24, 55), invertase (56), and acid phosphatase (25) are selectively secreted into the growing bud. Furthermore, newly synthesized mannoproteins have been shown to appear first at the bud tip (24, 55). We examined the insertion of newly synthesized mannoproteins into the cell wall by labeling the cell surface with fluorescent Con A, which binds mannose polymers. When the cells were allowed to grow further in the absence of label, newly inserted cell wall material appeared as a dark spot. In wild-type, *cap2Δ/cap2Δ*

mutant strains, and strains overexpressing capping protein, new growth occurred at the tip of the bud (Fig. 6).

Wild-type and *cap2Δ/cap2Δ* mutant populations had a similar proportion of cells exhibiting dark bud tips. In one experiment, 17/87 wild-type cells (20%) and 13/80 mutant cells (16%) had dark bud tips. Other cells had buds which were completely bright (9/87 = 10% for wild-type and 11/80 = 14% for mutant) or completely dark (61/87 = 70% for wild-type and 56/80 = 70% for mutant). The percentages of dark tips are not directly comparable because the strains were grown for different times (60 min for wild-type and 120 min for mutant) after the removal of the Con A label to allow for the disparity in growth rates between wild-type and mutant strains (5). In addition, these results do not exclude a partial defect in polarized growth because deposition of the appearance of some newly synthesized cell wall material would not be detected by this assay. Therefore, we also performed the following two assays, one on budding cells and one on mating cells, which do detect the polarized deposition of newly synthesized cell wall.

Chitin Deposition

Budding is preceded by the assembly of a ring of actin dots

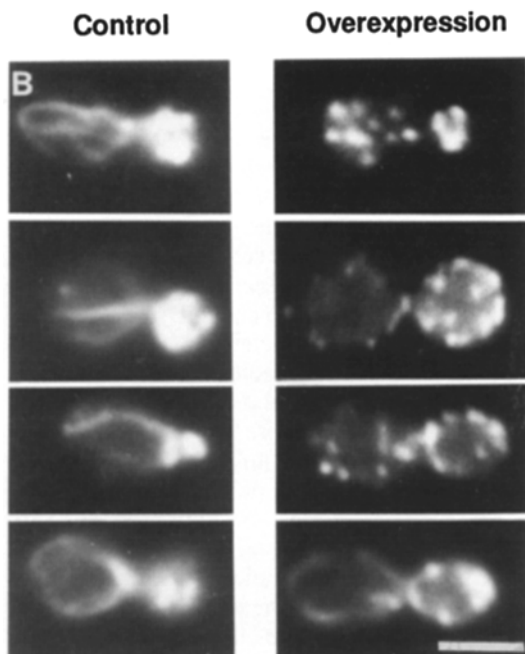
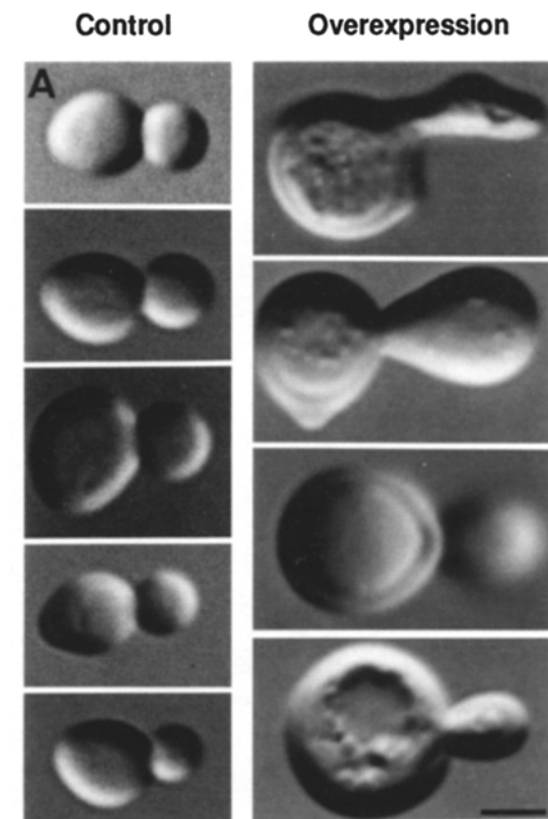


Figure 5. Overexpression of capping protein. (A) Morphology in control cells and cells overexpressing capping protein. (B) Actin distribution in a different set of control and overexpressing cells, which are not the same cells shown in A. The cell on the lower right in B is an example of the 5% of cells retaining actin cables under overexpressing conditions. Bars, 3 μ m.

and a ring of chitin at the presumptive bud site; after budding the chitin ring remains on the mother cell as a bud scar. Formation of the chitin ring requires chitin synthase 3 (53), and chitin deposition probably reflects the polarized transport of chitin synthase 3, or a factor that activates this enzyme (51). Capping protein null strains do synthesize chitin rings (Fig. 7). In wild type strains, chitin is also found at a low level over the surface of the mother, but not the bud (53). *cap2* Δ strains have relatively more chitin over the surface of the mother cell than do wild-type strains (Fig. 7 A) (5). Increased chitin deposition occurs in *cdc* mutants at the restrictive temperature, perhaps reflecting ongoing maturation in the absence of budding (53). Therefore, the increased chitin content of *cap2* Δ mother cell walls may simply reflect the prolonged cell cycle time of these strains. Consistent with this, we find that the largest cells in *cap2* Δ strains stain most brightly with Calcafluor (data not shown).

Fig. 7 also shows that bud site selection is correct in a null mutant. Haploids bud successively at one pole, and diploids alternate between the two poles with successive buds, leading to clustering of bud scars in wild-type cells. The bud scars also cluster in *cap2* Δ cells, indicating that bud site selection, under the control of the *BUD* genes (15, 16) is normal in these mutants. In diploid strains homozygous for the *cap2* deletion allele, the bud scars cluster at both poles (not shown).

Morphogenesis and Mating Efficiency

Haploid cells exposed to pheromone from a cell of the opposite mating type arrest in the G1 stage of the cell cycle and form projections in which actin dots are clustered at the tip (18) and chitin is deposited at the base (50). Haploids are able to discriminate among potential mating partners, suggesting that cells are able to spatially polarize their growth in response to gradients of mating pheromone (33). We tested whether capping protein null mutants are able to undergo normal morphogenesis and mating. A MAT α *cap1* Δ *cap2* Δ strain formed projections when exposed to synthetic α -factor, and actin dots clustered at the tip (Fig. 8). Chitin was correctly localized to the base of the projection (Fig. 9).

We also tested the mating efficiency of the mutant strains. When MAT α (YJC388) and MAT α (YJC096) wild-type cells were mixed, the efficiency of diploid formation was 48.3% \pm 1%. When MAT α *cap1* Δ *cap2* Δ mutant cells (YJC391) were mixed with MAT α wild-type cells (YJC096), the efficiency of diploid formation was 48.0% \pm 0.8%. Thus, *cap1* Δ *cap2* Δ mutant cells mate as efficiently as wild type. In a separate experiment, a small defect in mating was seen when both mating partners were capping protein mutants: MAT α *cap2* Δ (YJC078) and MAT α *cap2* Δ (YJC447) formed diploids with an efficiency of 29.6% \pm 1%, whereas MAT α *cap2* Δ (YJC078) and MAT α wild-type (YJC365) formed diploids with an efficiency of 40.9% \pm 2.5%. (The two experiments are not directly comparable because they were performed in different genetic backgrounds. For technical reasons we were unable to perform all three types of crosses in a uniform background.) The defect seen in mating of *cap2* Δ \times *cap2* Δ is much less severe than that seen in crosses of *tpm1* Δ \times *tpm1* Δ (39).

cap2 Δ mutants also demonstrated no significant defect in a mating partner discrimination assay (35) (R. Dorer and L. H. Hartwell, personal communication), which assesses the abil-

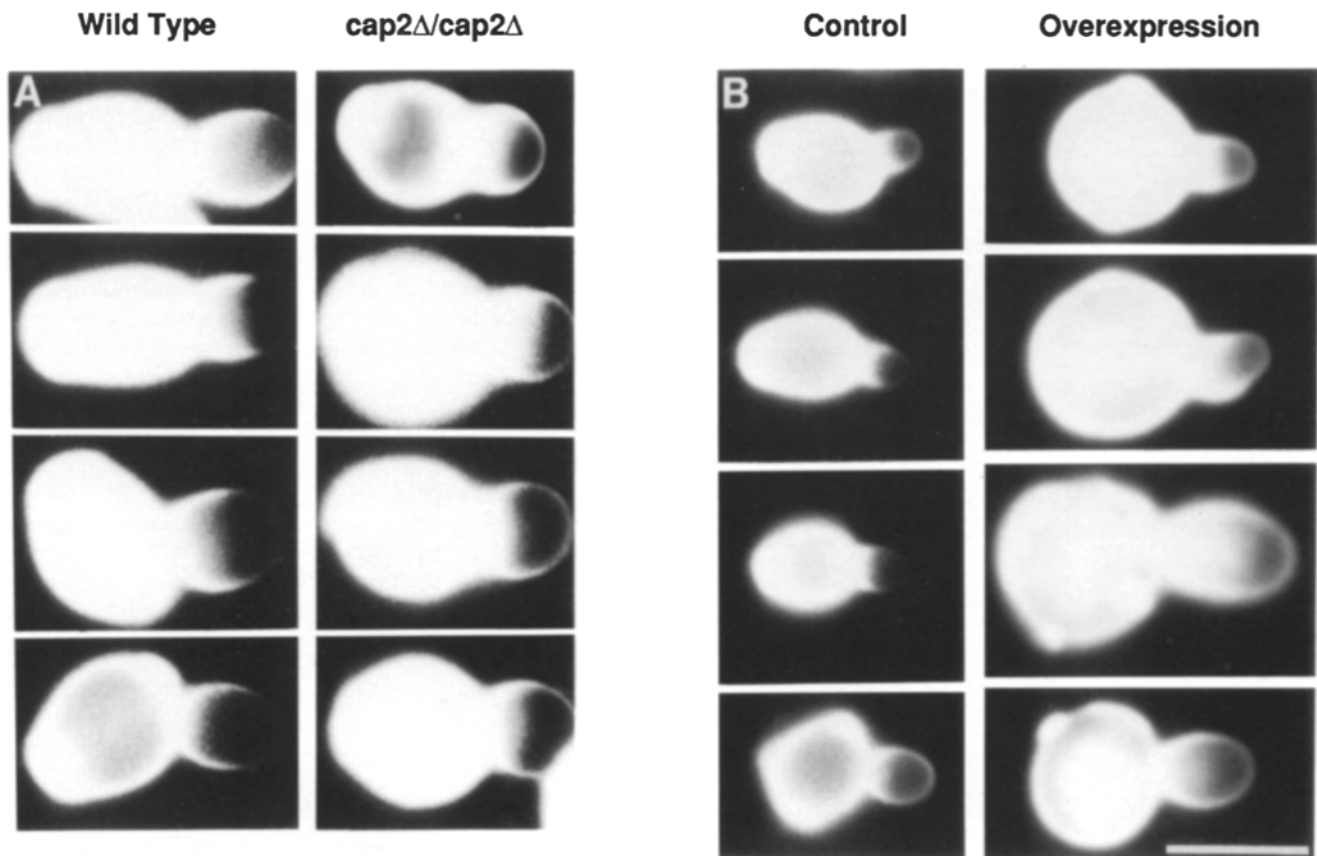


Figure 6. Polarized cell-wall growth in wild-type and capping protein null and overexpresser strains. Cells were labeled with fluorescein-Con A and allowed to grow further in the absence of label before viewing. New cell wall growth appears as a dark spot. (A) Wild-type (YJC163) vs. *cap2Δ* (YJC165). (B) Control (YJC285) vs. capping protein overexpresser (YJC288). The irregular profile of many of the mother cells is due to staining of bud scars by fluorescein-Con A. Bar, 5 μ m.

ity of a haploid cell to mate specifically with one of many possible partners. Thus, *cap1Δcap2Δ* mutant strains show little or no defect in polarization associated with mating.

Invertase Secretion

When budding yeast are grown in low-glucose media, a membrane-bound form of the enzyme invertase is induced and secreted (11, 12). In strains bearing temperature-sensitive alleles of the *ACT1* gene at the restrictive temperature, Novick and Botstein (42) found that derepressed invertase accumulated intracellularly, consistent with a role for actin in this secretion. When we examined invertase secretion in wild-type and *cap1Δcap2Δ* strains, we found that the mutant strains exhibited normal invertase secretion (Fig. 10), indicating that actin cables are not required for this process.

In wild-type cells, invertase is secreted selectively into the periplasmic space of the bud (56). On the other hand, invertase secretion continues in *myo2-66* strains at the restrictive temperature, conditions under which no bud is formed (36). Our assay does not distinguish the site of invertase secretion, and therefore invertase secretion may in this case represent bulk rather than polarized secretion.

Discussion

To understand the role of capping protein in the regulation

of the actin cytoskeleton and the function of the actin cytoskeleton in yeast, we have prepared null and overexpressing yeast strains of capping protein.

In previous work, the gene for the β subunit, *CAP2*, was cloned by serendipity, identified by sequence homology, and deleted (5). Purification and sequencing of capping protein confirmed that *CAP2* encodes the β subunit (6). We now report the cloning, sequencing and deletion of *CAP1*, the gene encoding the α subunit. Chickens contain two genes encoding different isoforms of the α subunit of capping protein (17), but we find no evidence for more than one gene in yeast. Negative evidence against this possibility includes the observations that an immunoblot with polyclonal antibodies is completely negative on extracts of null mutants, two-dimensional gel electrophoresis shows a single spot corresponding to the α subunit, and complete agreement between the properties of the protein and the prediction from *CAP1*.

The null mutants *cap1Δ CAP2*, *CAP1 cap2Δ*, and *cap1Δ cap2Δ* were prepared by deletion of nearly all the coding region by homologous recombination. The mutations are recessive, and haploid mutants are viable with a mild deficit in growth rate.

In a haploid, deletion of the gene for one subunit leads to a loss of protein for the other subunit, determined by immunoblot of whole cell extracts. Therefore, we hypothesize that single capping protein subunits are unstable in the absence of their heterodimeric partner. As expected from this observation, the phenotypes of each single mutant, *cap1Δ CAP2*

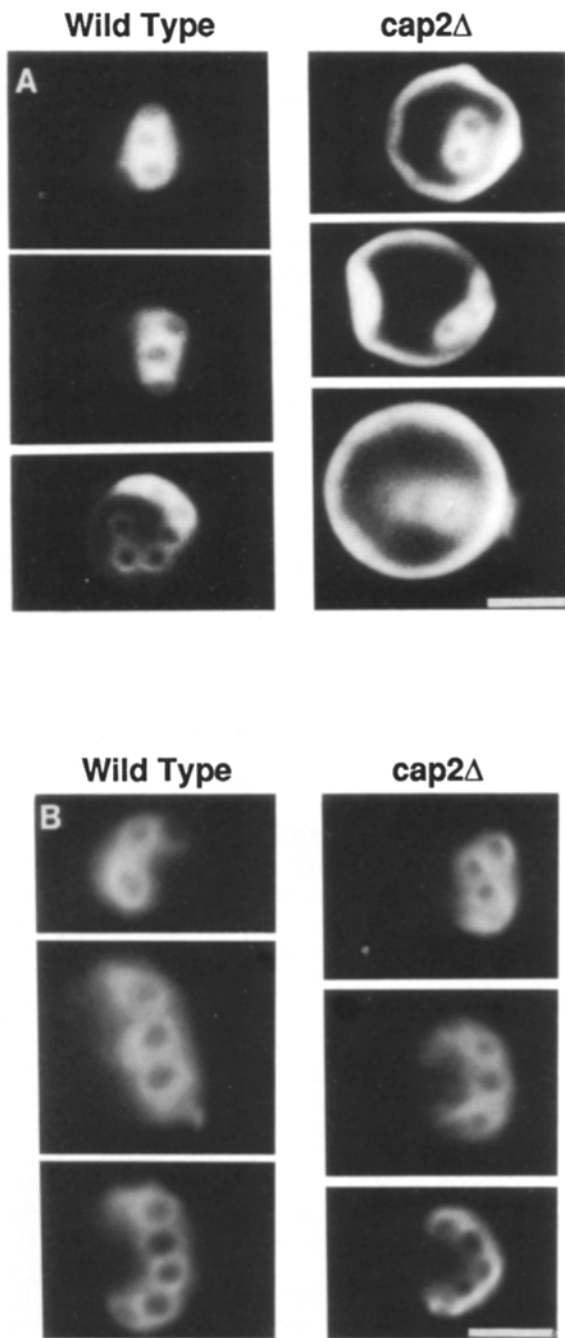


Figure 7. Chitin localization in wild-type and capping protein null strains. Asynchronously growing log-phase cells were stained with Calcafluor, washed, and observed. (*Wild-type*) YJC082; (*cap2Δ*) YJC085. Both *A* and *B* are from the same experiment; the difference is in the printing of the negative. (*A*) These images were photographed and printed under identical conditions, which demonstrates that mutants have chitin rings but also partial delocalization relative to wild-type. (*B*) Negatives were printed to display the pattern of the bud scars, which is similar in wild-type and mutant. Bar, 3 μm .

and *CAP1 cap2Δ*, are the same as each other and the same as the double mutant *cap1Δ cap2Δ*.

The null mutant strains have an altered actin cytoskeleton as characterized by fluorescence microscopy, including a loss of actin cables from the mother cell and the appearance of actin spots in a diffuse pattern over the cortex of the

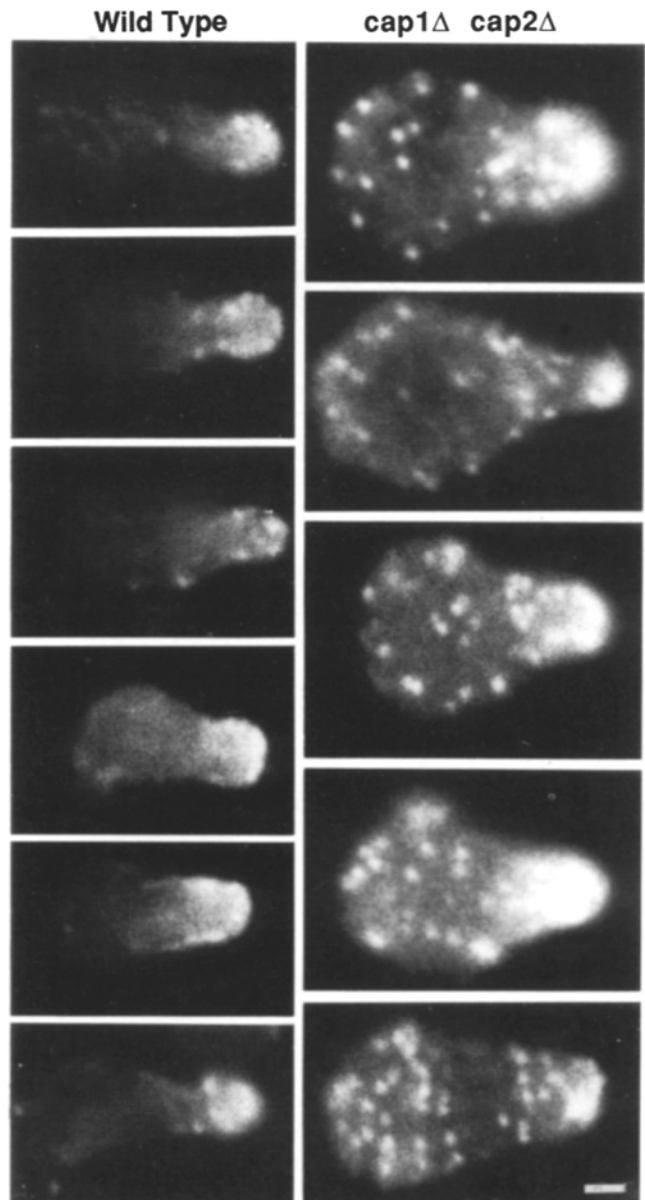


Figure 8. Actin distribution in wild-type and capping protein null strains exposed to mating pheromone. Cells were exposed to mating pheromone, fixed, and stained with rhodamine phalloidin. Mutant cells form projections, in which actin is concentrated, as do wild-type cells. (*Wild Type*) YJC093; (*cap1Δ cap2Δ*) YJC384. Bar, 1 μm .

mother and bud. These results suggest that capping protein is required for the stability of the actin structures comprising the cables. Based on its biochemical activity, capping barbed ends and nucleating polymerization, and immunofluorescence localization of capping protein to actin spots but not cables, it is unclear why the absence of capping protein should destabilize the cables or promote the diffuse localization of spots. In addition, overexpression of capping protein also leads to similar effects on the actin cytoskeleton, which is difficult to rationalize. Our lack of understanding about the structure, organization and dynamics of actin filaments in yeast severely limits our ability to explain these effects with specific mechanisms. One possibility is that a lack of capping protein destabilizes actin filaments in cables because capping protein is a component of cables, perhaps only at their

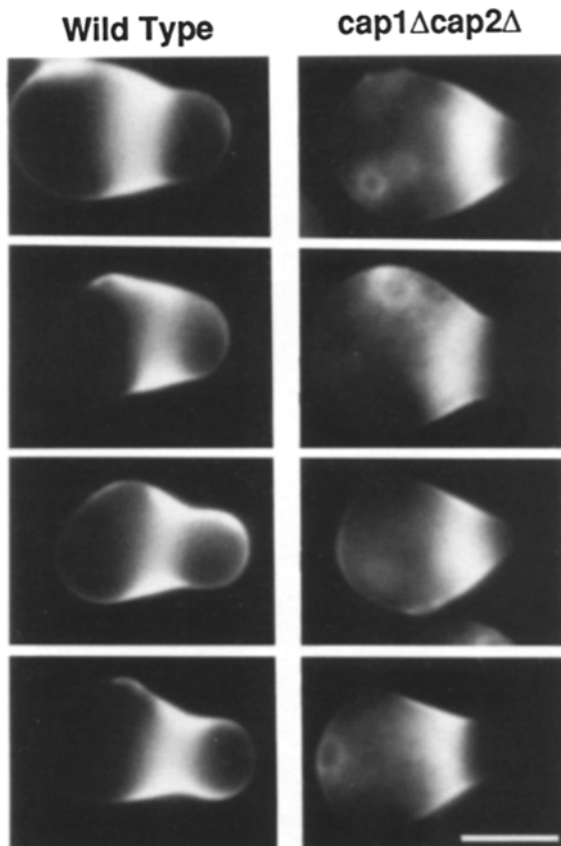


Figure 9. Chitin distribution in wild-type and capping protein null strains exposed to mating pheromone. Cells were exposed to mating pheromone, fixed, and stained with Calcafluor. Mutant cells localize a ring of chitin to the base of the projection, as do wild-type cells. (Wild-type) YJC093; (*cap1Δcap2Δ*) YJC384. Bar, 2 μ m.

ends, and that overexpression of capping protein nucleates the formation of many new short filaments, causing cables to depolymerize by mass action.

Polarized Secretion

Several phenomena probably reflect polarized secretion in yeast, and they may have different mechanisms. To begin the cell cycle, a bud site is chosen and a bud forms, reflected by the location of the chitin-containing bud scar. The bud enlarges, but not the mother, and growth occurs by the insertion of new cell wall material at the tip of the bud. This polarization of growth may be mediated by the directed transport of secretory vesicles from the mother cell into the bud (49). The mechanism of this transport is not known, but actin cables have been hypothesized to play a role in secretory vesicle transport because they run longitudinally along the mother bud axis and because they intersect the bud neck (20, 22, 36). In response to mating pheromone, cells from shmoo projections, which have chitin at their base. Actin cables also are oriented toward the projection. However, the results here argue against the hypothesis that cables are necessary for these various phenomena of polarized growth.

First, based on the insertion of newly synthesized cell wall material in *cap2Δ* strains, polarized cell wall growth occurs in cells deficient in cables. Second, disruption of cables by a different mechanism, overexpression of capping protein,

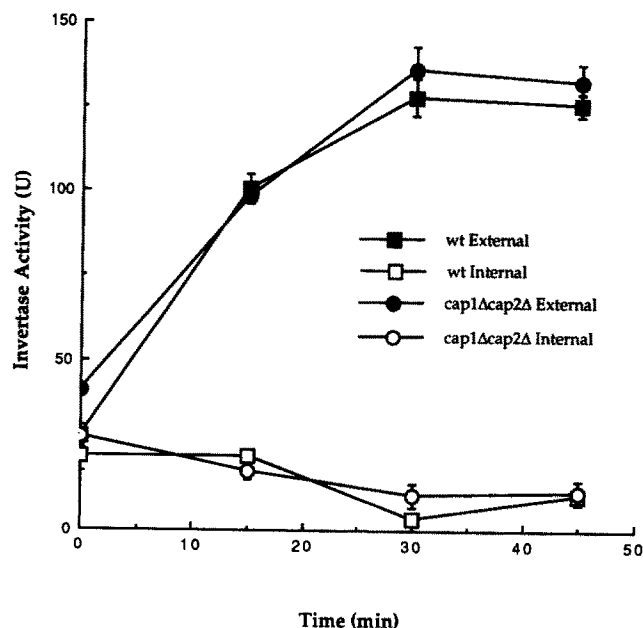


Figure 10. Invertase secretion in wild-type and capping protein null strains. Units of invertase activity (mean \pm SD, $n = 3$) is plotted against time after shift to 0.1% glucose. (■,●) External invertase; (□,○) internal invertase. (■,□) Wild-type (YJC388); (●,○) *cap1Δcap2Δ* (YJC391). Results for wild-type and mutant cells are similar.

also failed to disrupt the polarized insertion of new cell wall components at the bud tip. Third, capping protein null mutants deposited chitin in the bud scar and also at the neck of shmoos. Fourth, null strains undergo normal morphogenesis in response to mating pheromone and mate with an efficiency and discrimination similar to that of wild-type strains. Finally, invertase secretion and bud-site selection are also normal in the absence of cables.

We wish to emphasize that a general limitation of studying both null and overexpressing strains is that cells have ample time to adapt their metabolism and thereby correct physiologic defects, as demonstrated for clathrin heavy chain (52), for example. In the future, more definitive experiments to understand the role of capping protein and thereby that of actin will involve the preparation and analysis of conditional alleles.

The importance of actin in mediating polarized secretion is supported by several studies. Yeast with *ts* alleles of *ACT1* exhibit impaired secretion and delocalized chitin deposition at the permissive temperature and a loss of viability at the restrictive temperature (42). Temperature-sensitive mutations of *MYO2*, whose sequence contains the actin-based motor domain of myosin, cause yeast to arrest as large, unbudded cells (36) which indicates that *MYO2* is important for initiation of bud formation. Mating partner discrimination, which depends on the ability of mating cells to polarize their growth in a given direction, is impaired in *act1-2* and *act1-2* mutant cells (35). Clearly, actin is important for polarized secretion, but which pool of actin is required?

Spots are an obvious candidate because they contain actin and because the location of spots correlates with sites of new cell-surface growth (1). Mutants lacking spots have not been described. Strains lacking SAC6p (fimbrin), which like capping protein is localized to spots, still contain spots and are viable (2). Myosin-mediated vesicle transport should require

- Calcefluor. *Methods Enzymol.* 194:732-735.
45. Pringle, J. R., R. A. Preston, A. E. Adams, T. Stearns, D. G. Drubin, B. K. Haarer, and E. W. Jones. 1989. Fluorescence microscopy methods for yeast. *Methods Cell Biol.* 31:357-435.
 46. Rose, M. D., F. Winston, and P. Hieter. 1990. *Methods in Yeast Genetics: A Laboratory Course Manual.* Cold Spring Harbor Press, Cold Spring Harbor, NY.
 47. Sambrook, J., E. F. Fritsch, and T. Maniatis. 1989. *Molecular Cloning: A Laboratory Manual.* Cold Spring Harbor Laboratory Press, Cold Spring Harbor, NY.
 48. Sanger, F., S. Nicklen, and A. R. Coulson. 1977. DNA sequencing with chain terminating inhibitors. *Proc. Natl. Acad. Sci. USA.* 74:5463-5467.
 49. Schekman, R. 1985. Protein localization and membrane traffic in yeast. *Ann. Rev. Cell. Biol.* 1:115-143.
 50. Schekman, R., and V. Brawley. 1979. Localized deposition of chitin on the yeast cell surface in response to mating pheromone. *Proc. Natl. Acad. Sci. USA.* 76:645-649.
 51. Schekman, R., and P. Novick. 1982. The secretory process and yeast cell-surface assembly. *In The Molecular Biology of the Yeast Saccharomyces. Vol. II: Metabolism and Gene Expression.* Strathern, J. N., E. W. Jones, and J. R. Broach, editors. Cold Spring Harbor Press, Cold Spring Harbor, NY.
 52. Seeger, M., and G. S. Payne. 1992. A role for clathrin in the sorting of vacuolar proteins in the golgi-complex of yeast. *EMBO (Eur. Mol. Biol. Organ.) J.* 11:2811-2818.
 53. Shaw, J. A., P. C. Mol, B. Bowers, S. J. Silverman, M. H. Valdivieso, A. Duran, and E. Cabib. 1991. The function of chitin synthases 2 and 3 in the *Saccharomyces cerevisiae* cell cycle. *J. Cell Biol.* 114:111-123.
 54. Sikorski, R. S., and P. Hieter. 1989. A system of shuttle vectors and yeast host strains designed for efficient manipulation of DNA in *Saccharomyces cerevisiae*. *Genetics.* 122:19-27.
 55. Tkacz, J. S., and J. O. Lampen. 1972. Wall replication in *Saccharomyces* species: use of fluorescein-conjugated concanavalin A to reveal the site of mannan insertion. *J. Gen. Microbiol.* 72:243-247.
 56. Tkacz, J. S., and J. O. Lampen. 1973. Surface distribution of invertase in growing *Saccharomyces* cells. *J. Bacteriol.* 113:1073-1075.
 57. van Tuinen, E., and H. Riezman. 1987. Immunolocalization of glyceraldehyde-3-phosphate dehydrogenase, hexokinase and carboxypeptidase Y in yeast cells at the ultrastructural level. *J. Histochem. Cytochem.* 35:327-333.
 58. Wright, R., and J. Rine. 1989. Transmission electron microscopy and immunocytochemical studies of yeast: Analysis of HMB-CoA reductase overproduction by electron microscopy. *Methods Cell. Biol.* 31:473-512.